PARALLEL PLATE CAPACITIVE DETECTION OF LARGE AMPLITUDE MOTION IN MEMS

Alexander A. Trusov and Andrei M. Shkel
Department of Mechanical and Aerospace Engineering, University of California, Irvine,
Irvine, CA, USA
(Tel : +1-949-824-6314; E-mail: atrusov@uci.edu, ashkel@uci.edu)

Abstract: Detection of motion with parallel plate capacitors is commonly used in MEMS; small amplitude of motion is typically assumed. In this paper, we derive precise and constructive equations for the case of parallel plate capacitive detection of large amplitude of motion. These equations are solved in closed form without using a small displacement assumption. A precise relationship between the amplitude of the mechanical motion and the amplitude of the electrical sensing signals is obtained which allows the elimination of the nonlinearity error. To illustrate the theoretical findings, MEMS test structures were designed and fabricated. Experiments confirm the developed theory. The proposed algorithms of detection are especially valuable for capacitive detection of arbitrary amplitudes of motion in resonant structures such as gyroscopes, resonant microbalances, and chemical sensors.

Keywords: capacitive detection, parallel plates, EAM, MEMS resonant sensors

TRANSDUCERS & EUROSENSORS '07
The 14th International Conference on Solid-State Sensors, Actuators and Microsystems, Lyon, France, June 10-14, 2007

1. INTRODUCTION

Capacitive phenomena are commonly used for transduction in vibratory MEMS such as resonators [1], gyroscopes [2], fatigue and chemical sensors [3]. Capacitive detection of harmonic motion is often based on measuring the current induced by the relative motion of the capacitive electrodes. Parallel plates and lateral combs are the two most common configurations of capacitive structures used to actuate and detect motion in dynamic MEMS. Typically, for the same real estate, parallel plate sense capacitors provide a much higher capacitive gradient and thus sensitivity [4]. However, unlike lateral combs, parallel plates generate detection signals that are nonlinear with motional amplitude. Historically, this has limited the use of parallel plate capacitive detection to small amplitudes of motion, e.g., the sense mode of vibratory gyroscopes.

Electromechanical Amplitude Modulation (EAM) is a widely used capacitive detection approach. It is based on modulation of the motional signal by an AC probing voltage (carrier) and allows for frequency domain separation between the informational signals and feed-through of the driving voltages [5]. Conventional linear EAM demodulation can be used for either lateral comb sense capacitors or small displacement parallel plate capacitors. This work studies the application of the EAM technique to parallel plate detection of motion in vibratory devices with arbitrary motional amplitude. We derive precise equations for parallel plate capacitive detection and solve them directly in closed form without using small displacement assumptions. Signal processing algorithm that yields precise measurement of arbitrary amplitude of motion using parallel plates is proposed.

2. ELECTROMECHANICAL MODEL

Fig. 1 shows a general schematic of a capacitive microresonator, a basic element of various microsensors. The electro-mechanical diagram includes the mechanical resonator and the electrostatic drive and sense electrodes. The suspended mass of the resonator is constrained to move only along the horizontal x-axis. The variable sense capacitance is $C_s(x)$, and $C_d(x)$ is the drive capacitance. Typically in MEMS devices, drive and sense terminals are not completely isolated, but are electrically coupled by stray parasitic circuits [6]. In this paper, we assume without loss of generality that the parasitic circuit consists of a single lumped capacitor C_p. An AC driving voltage $V_d(t) = v_d \cos(\omega_d t)$ is applied to the drive electrode to actuate a harmonic motion.

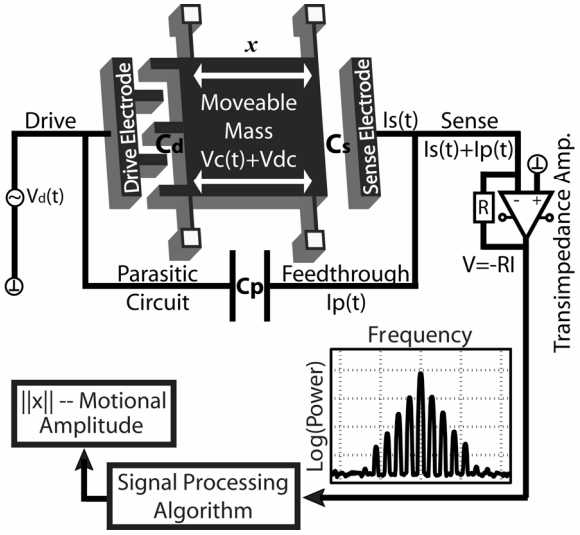

Fig. 1 Schematic of a capacitive MEMS resonator.

The sense capacitor $C_s(x)$ is formed between the mobile mass and the fixed sense electrode, which is connected to the inverting input of a trans-impedance amplifier. The oscillatory motion of the resonator is excited by the electrostatic force in the drive capacitor. Without discussing further details of the actuation scheme, displacement $x(t)$ can be expressed as

$$x(t) = \| x \| \sin(\omega_d t + \phi). \quad (1)$$

Due to the motion, the sense capacitance $C_s(x)$ changes, causing a flow of motional current $I_s = d(C_s(t)V_s(t))/dt$, where $V_s(t)$ is the voltage across the sense capacitor. The total pick-up current $I(t) = I_s(t) + I_p(t)$ consists of both the motional and the parasitic currents and is converted to the final output voltage $V(t) = -RI(t)$. Parasitic current is induced by the drive voltage $V_d(t)$ and therefore has the same frequency ω_d. The total sensing voltage $V_s(t) = V_{dc} + V_c(t)$ is composed of a DC component and an AC component, called carrier. This configuration results in the EAM modulation of the motional signal. The total pick-up EAM voltage is given by

$$V(t) = -R\frac{d}{dt_s}\left[V_d(t)C_p + \left(V_c(t) + V_{dc}\right)C_s(t)\right]. \quad (2)$$

Depending on the particular form of the sense capacitance $C_s(x)$, Eq. (2) can be expanded to describe specific properties of the pick-up signal.

3. PARALLEL PLATE SIGNAL

Consider a variable sense capacitor $C_s(x)$ formed by a pair of mobile and anchored parallel plate structures. We denote media permittivity by ε, the initial gap between plates at rest by g, parallel plate pair overlap length L, and plate height (structural layer thickness) is y. The total overlap area in the capacitor is given by $A = NLy$, where N is the total number of parallel plate pairs in the capacitive structure. For the motion described by Eq. (1), the total variable sense capacitance is

$$C_s(t) = \frac{\varepsilon A}{g - x(t)} = \frac{\varepsilon A}{g}\frac{1}{1 - \frac{\|x\|}{g}\sin(\omega_d t)}, \quad (3)$$

where the phase of motion ϕ is omitted without any loss of generality. We introduce nominal sense capacitance $C_{sn} = \varepsilon A/g$ and dimensionless amplitude of motion $x_0 = \|x\|/g < 1$. From Eq. (3), the sense capacitance is

$$C_s(t) = C_{sn}/\left(1 - x_0 \sin(\omega_d t)\right). \quad (4)$$

The Fourier series representation for the parallel plate capacitance $C_s(t)$ for a given amplitude of harmonic motion x_0 is

$$C_s(t) = C_{sn}\sum_{k=0}^{\infty} p_{2k}(x_0)\cos(2k\omega_d t) + C_{sn}\sum_{k=0}^{\infty} p_{2k+1}(x_0)\sin((2k+1)\omega_d t), \quad (5)$$

where functions $p_k(x_0)$ define the amplitudes of the multiple harmonics in the capacitance $C_s(t)$. For $k = 1, 2...$ these functions are given by

$$\|p_k(x_0)\| = \frac{2}{\sqrt{1 - x_0^2}}\left(\frac{x_0}{1 + \sqrt{1 - x_0^2}}\right)^k. \quad (6)$$

When parallel plates are used to detect harmonic motion, the time varying sense capacitance contains an infinite number of motional frequency harmonics. In order to calculate the total output signal, we consider EAM modulation of each capacitive harmonic individually. We combine the sense capacitance Eq. (5) with Eq. (2) to calculate the total output current:

1-4244-0842-3/07/$20.00©2007 IEEE

$$I(t) = -C_d v_d \omega_d \sin(\omega_d t) + C_{sn} v_c \omega_c p_0(x_0)\cos(\omega_c t) +$$
$$+C_{sn} V_{dc} \omega_d \left\{ \begin{array}{l} \sum_{k=0}^{\infty} (2k+1) p_{2k+1}(x_0)\cos((2k+1)\omega_d t) - \\ \quad - \sum_{k=1}^{\infty} 2k p_{2k}(x_0)\cos(2k\omega_d t) \end{array} \right. \qquad (7)$$
$$+\frac{1}{2} C_{sn} v_c \sum_{k=0}^{\infty} p_{2k+1}(x_0) \left[\begin{array}{l} \omega_{2k+1}\sin(\omega_{2k+1} t) - \\ \quad - \omega_{-(2k+1)}\sin(\omega_{-(2k+1)} t) \end{array} \right]$$
$$+\frac{1}{2} C_{sn} v_c \sum_{k=1}^{\infty} p_{2k}(x_0)\left[\omega_{2k}\cos(\omega_{2k} t) + \omega_{-2k} c\,\mathrm{os}(\omega_{-2k} t)\right]$$

where, for arbitrary k, $\omega_k = \omega_c + k\omega_d$ is the frequency of the $|k|^{-th}$ order sideband (left or right, depending on the sign of k). Eq. (7) gives the Fourier series of the total pick-up signal for parallel plate capacitive detection of harmonic motion. Fig. 2 shows the frequency domain representation of a typical parallel plate EAM pick-up signal and illustrates its important features (in this example, the drive and carrier frequencies are 1 kHz and 20 kHz respectively).

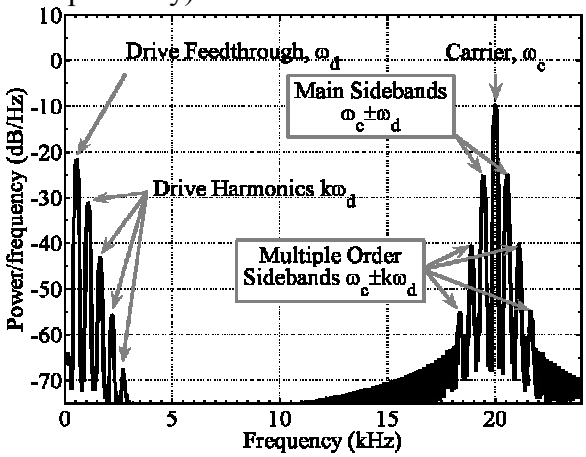

Fig. 2 Frequency spectrum of the parallel plate EAM pick-up signal (simulation).

Let V_ω denote harmonic component of an arbitrary frequency ω of the total output voltage. According to Eq. (7), the amplitudes of the right and left sidebands in the total output voltage are given by

$$\left\| V_{\omega_{\pm k}} \right\| = \frac{1}{2} R C_{sn} v_c \left\| (\omega_c \pm k\omega_d) p_k(x_0) \right\|. \qquad (8)$$

In practice, a high frequency carrier is usually used, so that $\omega_c \gg k\omega_d$ for several first orders $k = 1, 2, 3 \ldots K$. For these sidebands,

$$\left\| V_{\omega_{\pm k}} \right\| \approx \frac{1}{2} R C_{sn} v_c \omega_c \left\| p_k(x_0) \right\|. \qquad (9)$$

According to Eq. (6), the normalized amplitudes of multiple sidebands form a geometric progression with ratio

$$r(x_0) = \frac{\left\| p_{k+1}(x_0) \right\|}{\left\| p_k(x_0) \right\|} = \left(\frac{x_0}{1 + \sqrt{1 - x_0^2}} \right). \qquad (10)$$

This ratio is uniquely related to the amplitude of motion x_0.

4. PARALLEL PLATE DETECTION

Arbitrary amplitude of motion using parallel plate EAM signal can be precisely detected using the following procedure:

1) Mix the pick-up signal with a phase shifted carrier signal $V(t) \otimes \sin(\omega_c t)$ to map the sidebands from $\omega_c \pm \omega_d$ frequencies to ω_d frequency.

2) Mix the resulting signal with $\sin(\omega_c t + \alpha)$ to map the signal from ω_d frequency to DC, and low pass filter to attenuate remaining AC components in the signal.

3) Scale the obtained DC signal by $\left(RC_{sn} v_c \omega_c\right)^{-1}$. In the linear case, this completes the measurement procedure. In the parallel plate case an extra step is needed to compensate for the nonlinearity of $p_1(x_0)$.

4) The amplitude of motion is calculated precisely from the measured DC representation of the main sidebands normalized amplitude p_1:

$$x_0(p_1) = \frac{\left(w^2 - 12 + p_1^2\right)^2 - \left(p_1 w\right)^2}{18 p_1 w^2}, \qquad (11)$$
$$w = \left[72 p_1 - p_1^3 + 6\left(48 + 132 p_1^2 - 3 p_1^4\right) \right]^{1/6},$$

which is based on solving Eq. (6) for the amplitude of motion x_0. Alternatively, the amplitude of motion can be extracted by measuring the ratio of multiple sidebands and solving Eq. (10).

5. EXPERIMENTAL DEMONSTRATION

Fig. 3 shows an SEM micrograph of a test structure, which is a capacitive MEMS resonator with lateral comb and parallel plate drive and

sense capacitors. The fabrication was done using in-house wafer level SOI process. During the experiments, the device was driven into linear vibrations of different amplitudes at the resonant frequency of 555 Hz using the lateral comb drive capacitor. An AC carrier voltage at 20 kHz was applied to the mobile mass.

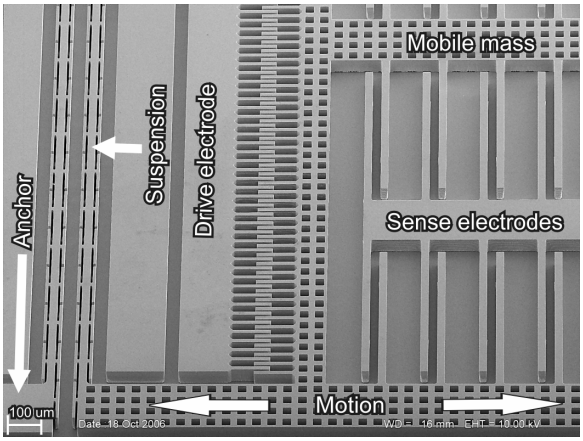

Fig. 3 SEM micrograph of a quarter of the fabricated test device.

Fig. 4 shows the frequency spectrum of the detection signal at different amplitudes of motion. As predicted by theory, multiple order sidebands are present in the spectrum and their amplitudes indicate the amount of mechanical motion. Fig. 5 shows a direct experimental measurement of the two first order sidebands at different amplitudes of motion.

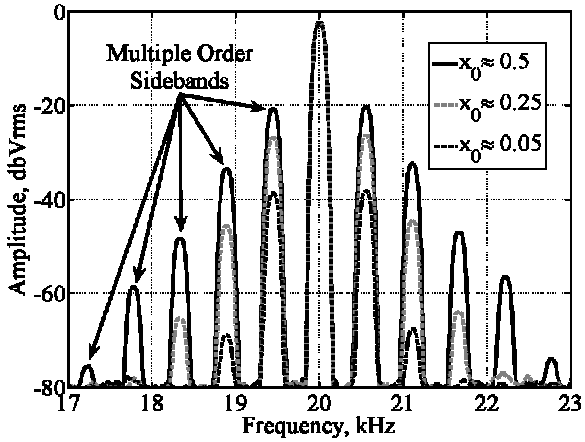

Fig. 4 Experimental measurement of the parallel plate EAM spectra.

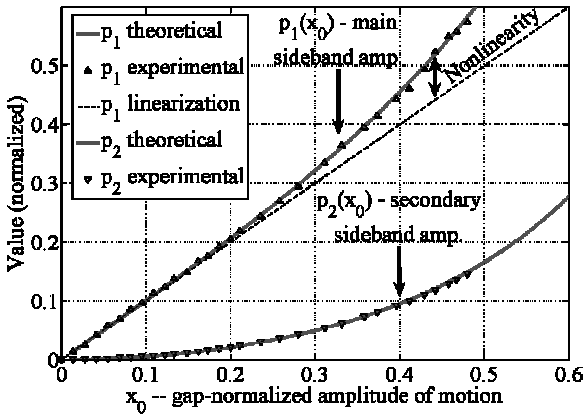

Fig. 5 Experimental measurement of the parallel plate EAM nonlinear sidebands.

6. CONCLUSIONS

In this paper theory and method of parallel plate detection of arbitrary amplitude of motion are developed and experimentally confirmed.

ACKNOWLEDGEMENTS

This work was supported by the National Science Foundation Grant CMS-0409923, BEI Technologies contract BEI-36974, and UC Discovery program ELE04-10202.

REFERENCES

[1] G. Stemme, "Resonant Silicon Sensors," IOP J. Micromech. Microeng., vol. 1 , pp. 113-125, 1991.

[2] N. Yazdi, F. Ayazi, and K. Najafi, "Micromachined Inertial Sensors," Proc. IEEE, pp. 1640-1659, Aug 1998.

[3] K. K. Turner and W. Zhang, "Design and Analysis of a Dynamic MEM Chemical Sensor," Proc. of the American Control Conference, 2001.

[4] W. A. Clark, "Micromachined Vibratory Rate Gyroscopes," Ph.D. thesis, UC Berkley, 1997.

[5] C. C. Nguyen, "Micromechanical Signal Processors," Ph.D. thesis, UC Berkley, 1994.

[6] A. Trusov, C. Acar, and A. M. Shkel, "Comparative Analysis of Distributed Mass Micromachined Gyroscopes Fabricated in SCS-OI and EFAB," Proceedings of SPIE, Smart Structures and Materials 2006, vol. 6174.